Review Article

CT cinematic rendering for pelvic primary tumor photorealistic visualization

Jun Yang, Kun Li, Huiyuan Deng, Jun Feng, Yong Fei, Yiren Jin, Chengde Liao, Qinqing Li

Department of Radiology, The Third Affiliated Hospital of Kunming Medical University, Yunnan Cancer Hospital, Kunming 650118, China

Correspondence to: Qinqing Li; Chengde Liao. Department of Radiology, The Third Affiliated Hospital of Kunming Medical University, Yunnan Cancer Hospital, No. 519 Kunzhou Road, Xishan District, Kunming 650118, China. Email: qinqing_81@163.com; 846681160@qq.com.

Abstract: Pelvic tumors can be both complicated and challenging, and computed tomography (CT) has played an important role in the diagnosis and treatment planning of these conditions. Cinematic rendering (CR) is a new method of 3D imaging using CT volumetric data. Unlike traditional 3D methods, CR uses the global illumination model to produce high-definition surface details and shadow effects to generate photorealistic images. In this pictorial review, a series of primary pelvic tumor cases are presented to demonstrate the potential value of CR relative to conventional volume rendering (VR). This technique holds great potential in disease diagnosis, preoperative planning, medical education and patient communication.

Keywords: Cinematic rendering (CR); pelvic tumor; imaging; computed tomography (CT)

Submitted Jul 25, 2018. Accepted for publication Sep 21, 2018.
doi: 10.21037/qims.2018.09.21
View this article at: http://dx.doi.org/10.21037/qims.2018.09.21

Introduction

At present, computed tomography (CT) is widely used in clinical practice with improvements in its resolution and image quality being made over recent decades. In addition to these advancements, the increase in computing power has made the more demanding visualization algorithms possible. For instance, volumetric data obtained from routine scans can now be reconstructed in 3D visualization. Currently, two types of 3D rendering techniques are commonly used to visualize volumetric 3D data: surface shaded display (SSD) and volume rendering (VR). These techniques provide a global overview of volumetric data, along with detailed anatomical and pathological information which is usually more difficult to discern in conventional 2D images (1). SSD is considered to be the predecessor of the VR technique (VRT) and uses simple attenuation threshold segmentation to identify and display the surface of the object. Meanwhile, VRT forms images based on volumetric data and assigns different colors and transparency to different attenuations (2). Another new imaging method, cinematic rendering (CR), which is not yet in clinical use, is capable of 3D visualization of volumetric data. One improvement of CR compared with traditional VR is the use of a photo-editing spherical panorama to illuminate the scanned object (3). CR uses a global lighting model and direct and indirect lighting to create an image for rendering quality (4). This novel technology provides detailed photorealistic visualization of high-density objects, including contrast-enhanced blood vessels, vascularized structures, tissues, organs, and bones (1). Although some pioneering studies have demonstrated that CR exhibits great prospects in clinical application (1,5-7), these studies were mainly performed to assess the cardiovascular system, abdominal organs, and traumatic fractures, and have not been performed for bone tumors, especially pelvic ones.

In this pictorial review, we discuss the role of CR in primary pelvic tumors and provide examples compared with VRT, demonstrating that CR is helpful in the diagnosis and evaluation of pelvic bone tumors. For our data, volumetric CT data were obtained from standard protocol on Siemens CT scanners (SOMATOM Definition AS or SOMATOM Force) and thin-slice images (1 mm) were reconstructed from 0.6 mm isotropic voxels. This volumetric raw data was

then used to create VR and CR images. VR reconstructions were created at a multimodality workstation (syngo.via, version VB10B, Siemens, Erlangen, Germany), and CR images were created with prototype software (syngo.via Frontier, version 1.2.0) in this workstation.

Normal pelvic anatomy

The pelvis consists of the left and right hips, sacrum and coccyx. CR produces cinematic images that can more clearly present the complex anatomy of the pelvis. *Figure 1* illustrates the normal pelvic anatomy as observed on CR and VR images. The hip bone is composed of the ilium, ischial and pubis bone. The acetabulum, a fusion of these three bones on each lateral side, is the site where the femoral head is located. The ilium is the largest of the three bones and is located in the upper part of the hip bone. The ischium is located in the lower back of the hip and can be divided into two parts, the body and the ramus. The ischial tuberosity is formed at the back of the body and the ramus, which is the sitting point for the weight of the sitting position. The ischial tuberosity is the lowest part of the ischium and can be observed on the body surface. CR presents 3D photorealistic anatomy of the pelvis from different angles and provides different view settings. In addition to observing the pelvic bone, CR can also clearly and intuitively observe pelvic vessels. It is easy to observe the variability of the blood vessels, the artery providing blood supply to the tumor, and the adjacent relationship between the tumor and blood vessels. The abdominal aorta to the lower edge of the fourth lumbar vertebral body is divided into the left and right common iliac artery; the common iliac artery is divided into the iliac crest and the external artery at the sacroiliac joint height. The two branches of the external iliac artery that can also be identified on the CR are the inferior epigastric artery and the deep iliac artery. Furthermore, CR can provide more anatomical information for the assessment of congenital pelvic anomalies.

Primary malignant pelvic tumors

Primary malignant pelvic tumors are not uncommon and include two main types: sarcomas, such as chondrosarcoma, osteosarcoma and Ewing's sarcoma; and hematological malignancies, such as lymphoma, multiple myeloma and plasmacytoma.

Chondrosarcoma

Chondrosarcoma is the most common primary malignant tumor of the pelvic bone, accounting for approximately 32% of cases, and is characterized by malignant proliferation of the cartilage-like matrix (8). Chondrosarcomas are most commonly located in the ilium and acetabulum. Chondrosarcoma is resistant to chemotherapy and radiation therapy, and extensive local excision is the only treatment. Imaging studies of the extent of the lesion are particularly important. The imaging performance of chondrosarcoma depends on the grade of the lesion. Low-grade lesions are typically small and often intraosseous with mild expansion of the cortical bone, and have clear boundaries, clear cartilage mineralization, and no soft tissue mass. High-grade chondrosarcoma often presents with expansive bone destruction, contains a large number of tumor stroma, and is surrounded by various calcifications and soft tissue masses. CR provides the tumor location from different angles, which helps surgeons to conceive the operation mode prospectively. Moreover, CR can vividly display various forms of calcification, such as amorphous and irregular calcification, and can completely reveal the panorama of calcifications (*Figure 2*).

Osteosarcoma

Osteosarcoma shows a bimodal age distribution. The first peak occurs in adolescents, and the second peak occurs in the elderly (9). Pelvic osteosarcoma is rare, accounting for only 7.2% of patients with osteosarcoma (10). Osteosarcoma, which occurs in the pelvis, is typically located at the back of the iliac wing and expands into the sacrum and lower lumbar spine (11). Osteosarcoma often presents with bone destruction, tumor bone formation and periosteal reactions. Tumor bone typically is fluffy and amorphous and exhibits cloud-like mineralization characteristics of osteoid matrix production. Codman triangles appear when the soft tissue components of the tumor cause the periosteum to bulge and be destroyed. Pelvic osteosarcoma is often accompanied by a soft tissue mass. Pelvic osteosarcoma is more often extended across the sacroiliac joint and hip joints compared with the extremities (12). CR can display the extensive tumor neovascularity and relationship with feeding vessels with different setting windows, which are important in presurgical planning (*Figure 3A,B,C*). CR images provide an even greater

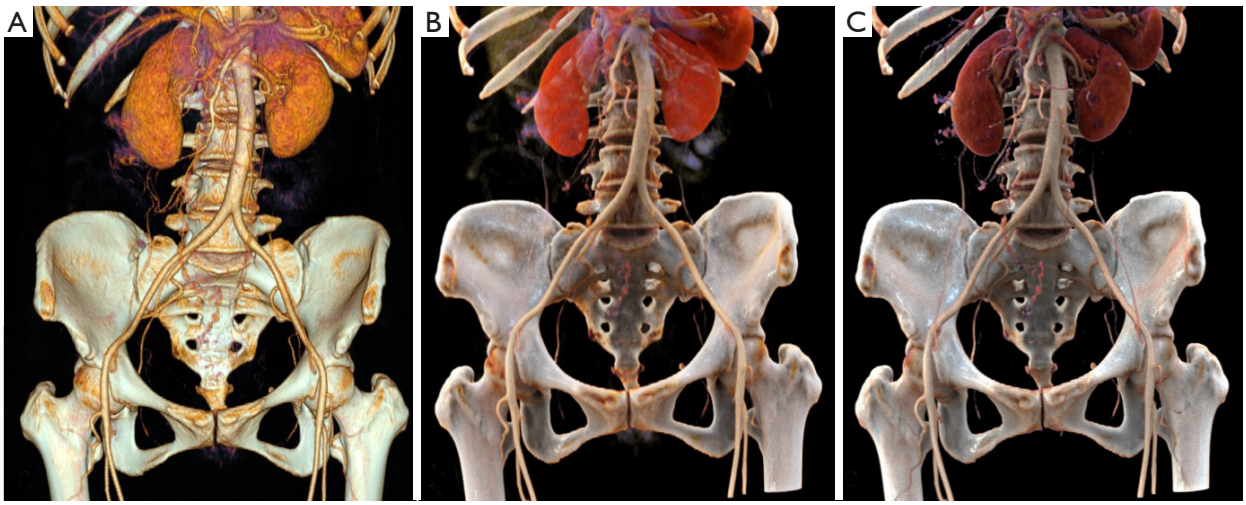

Figure 1 Normal pelvic anatomy. (A) VR; (B,C) CR with different window levels and width settings. VR, volume rendering; CR, cinematic rendering.

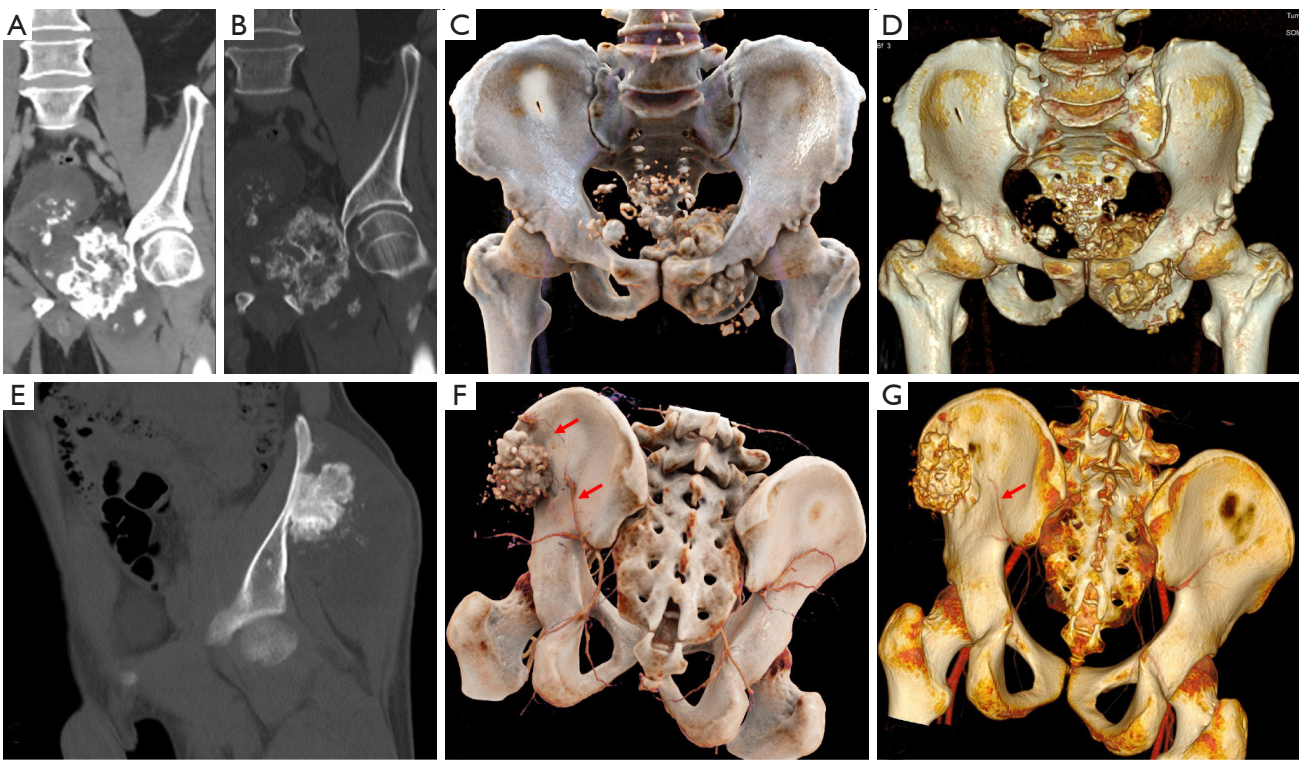

Figure 2 (A-D) Left superior branch of a pubis chondrosarcoma grade 2. A 59-year-old male presented with left lower extremity pain for 1 year that was aggravated for 1 month. The CT image shows a large destructive mixed mass arising from the left superior branch of the pubis, and a huge irregular soft tissue mass surrounds the mass (A,B). CR (C) demonstrated scattered patches, spots and circular calcification in the tumor more realistically than VR (D). (E-G) Left iliac wing chondrosarcoma grade 3. A 19-year-old male presented a left iliac progressive mass with pain for 3 months that was aggravated at night. The left iliac wing exhibited bone destruction, and multiple ring-shaped cartilaginous calcifications were found in the mass (E). CR (F) and VR (G) can evaluate lesions and their vessels from different angles, and CR shows these more clearly (red arrows). CT, computed tomography; CR, cinematic rendering; VR, volume rendering.

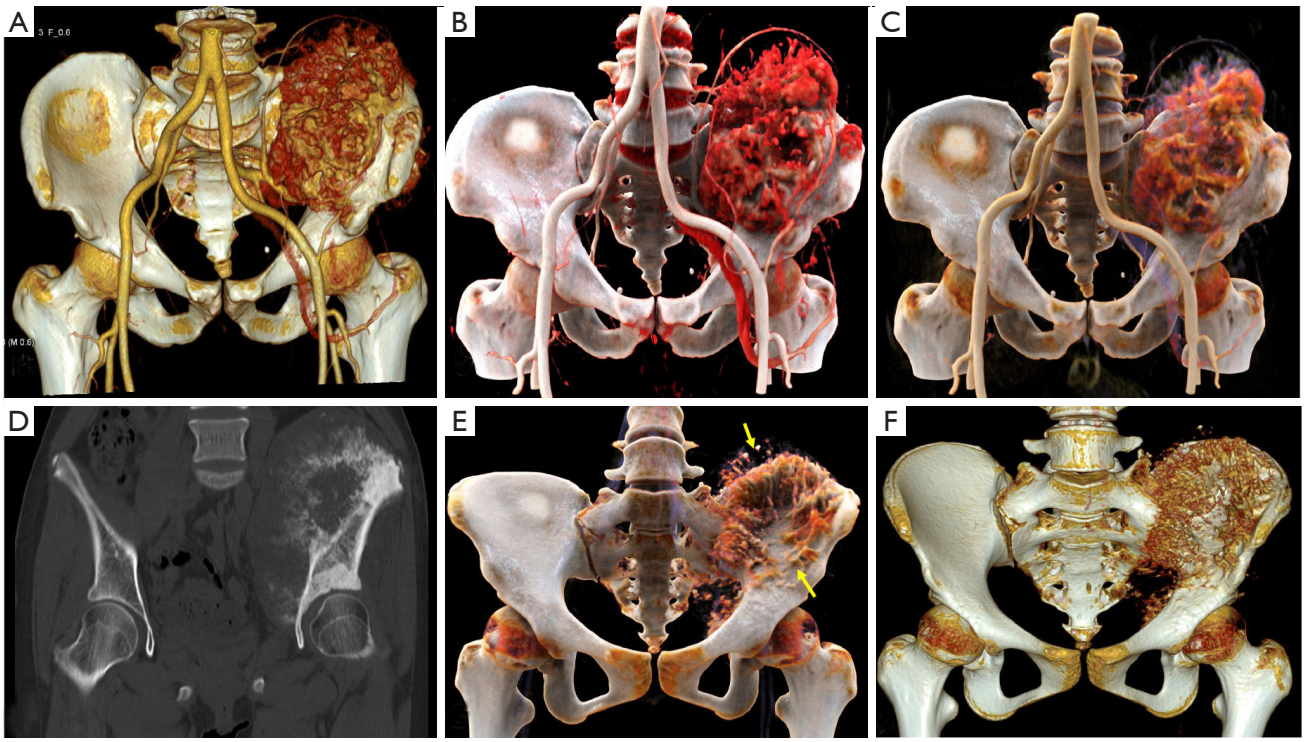

Figure 3 (A-C) A 49-year-old male presented with left ilium lumber pain for 2 months. The left iliac bone was extensively damaged by a huge soft tissue mass that extended to the left iliopsoas and glutaeus. A large number of tumor bones were observed in the mass, and a needle-like periosteal reaction was observed on the surface of the iliac bone. The left iliac bone was involved, but the bony structure of the sacral joint surface was normal. Most of the soft tissue masses exhibited significant inhomogeneous enhancement. Vessel contour is smoother on CR (B,C) compared to VR (A). (D-F) A 14-year-old female presented with left hip pain for 1 month that was aggravated with swelling for two weeks. The entire left iliac and acetabular destruction exhibited the ivory-like change (yellow arrows) (D). The density was inhomogeneous, and the lesion involved the sacroiliac and hip joint. The mass boundary was ill defined, and intratumoral radial high-density tumor bone was observed in CR (E) and VR (F). The pathological result was chondrocyte osteosarcoma. CR, cinematic rendering; VR, volume rendering.

level of detail, and CR presents a more realistic and vivid appearance of the tumor bone (*Figure 3D,E,F*).

Ewing's sarcoma

Ewing's sarcoma is a malignant, small, round, blue-cell tumor of the bone and soft tissue. Ewing's sarcoma is the second most common bone malignancy in children and adolescents, often occurring in the pelvis. Imaging findings include moth-eaten appearance, permeative bone destruction, onion skin features or thorn-like periosteal reaction with soft tissue masses (13). Due to the irregular pelvic morphology, Ewing's sarcoma that occurs in the pelvis rarely exhibits typical onion skin-like changes. The soft tissue mass around the tumor is typically larger than the bone destruction area, and the tumor margin is often ill defined and infiltrative. CR is beneficial for observing sacroiliac joint involvement and formulating the virtual pelvic reconstruction plan (*Figures 4,5*).

Multiple myeloma (MM) and plasmacytoma

MM is a malignant plasma cell disease that originates in plasma cells in the bone marrow and primarily involves the midshaft bone, especially in the spine, pelvis and skull. Bone destruction occurs as a result of the proliferation of plasma cells distributed in the bone marrow. The flat bones (vertebral bodies, skulls, pelvis) are particularly vulnerable as these bones contain a large amount of red bone marrow. Plasmacytoma is a solitary lesion that is similar to myeloma

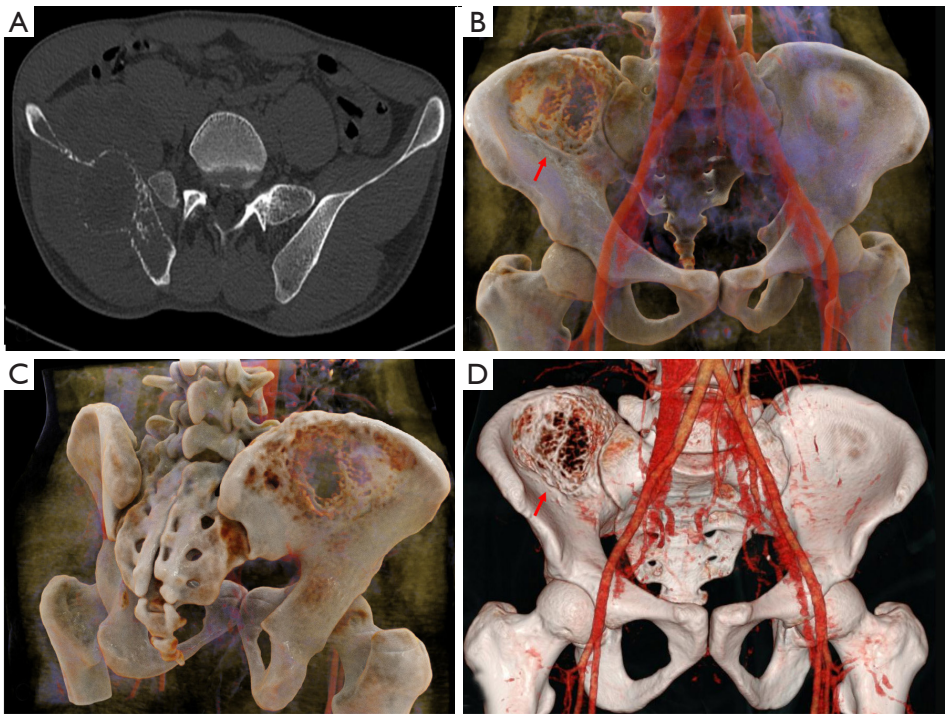

Figure 4 A 33-year-old male presented with right hip pain for more than one year (obvious at night) that was aggravated with numbness of the lower extremities and activity disorder for 3 weeks. 2D CT image (A), CR (B and C) and VR (D) show that the right iliac bone exhibits widespread osteolytic destruction, and the edge is well defined (red arrows). Contiguous spread of this mass is not across the sacroiliac joint into the right sacrum. CT, computed tomography; CR, cinematic rendering; VR, volume rendering.

with large numbers of plasma cells. Plasmacytoma is generally considered an early manifestation of multiple myeloma, so the prognosis is better. Imaging findings include diffuse osteoporosis, osteolytic bone destruction, and no hardening of the edges. The lesions are separated from each other and are similar in size. On an X-ray of the skull, plasmacytoma appears as "punched-out" lesions. Compression fracture of the vertebral body and soft tissue mass is typically observed on CT. CR and VR can be used to observe the lesions in a comprehensive manner, and CR offers superior details and pathological fractures (*Figures 6*,*7*).

Lymphoma

Primary non-Hodgkin lymphoma (PHL) very rarely occurs in bone. PHL arises in the diaphysis of long bones or in flat bones of the axial skeleton. PHL also includes small round cell tumors that rarely occur in the pelvic region and tends to occur in older ages (8). Imaging findings include osteolytic bone destruction, subtle cortical destruction, and periosteal reactions, and show normal tissue surrounded by tumor: all similar imaging findings to Ewing's sarcoma. However, the soft tissue masses are smaller than Ewing's sarcoma, and sclerosis may be more prominent (14). Lymphoma that occurs in the vertebral body can involve intervertebral discs and continuous vertebral bodies. The relationship between tumor and pelvic blood vessels can be clearly displayed on CR at different levels, and vascular and bone destruction can be observed simultaneously (*Figure 8*).

Chordoma

Chordoma is a slow-growing, low-grade malignant tumor that originates from the hereditary spinal cord remnant at the end of the spine (15). Most of the chordomas that occur in the pelvis are found in the sacrum, especially the fourth and fifth sacral vertebra. Imaging findings include lytic destruction in the inferior portion of the sacrum and coccyx and a clear boundary of the mass without an osteosclerotic

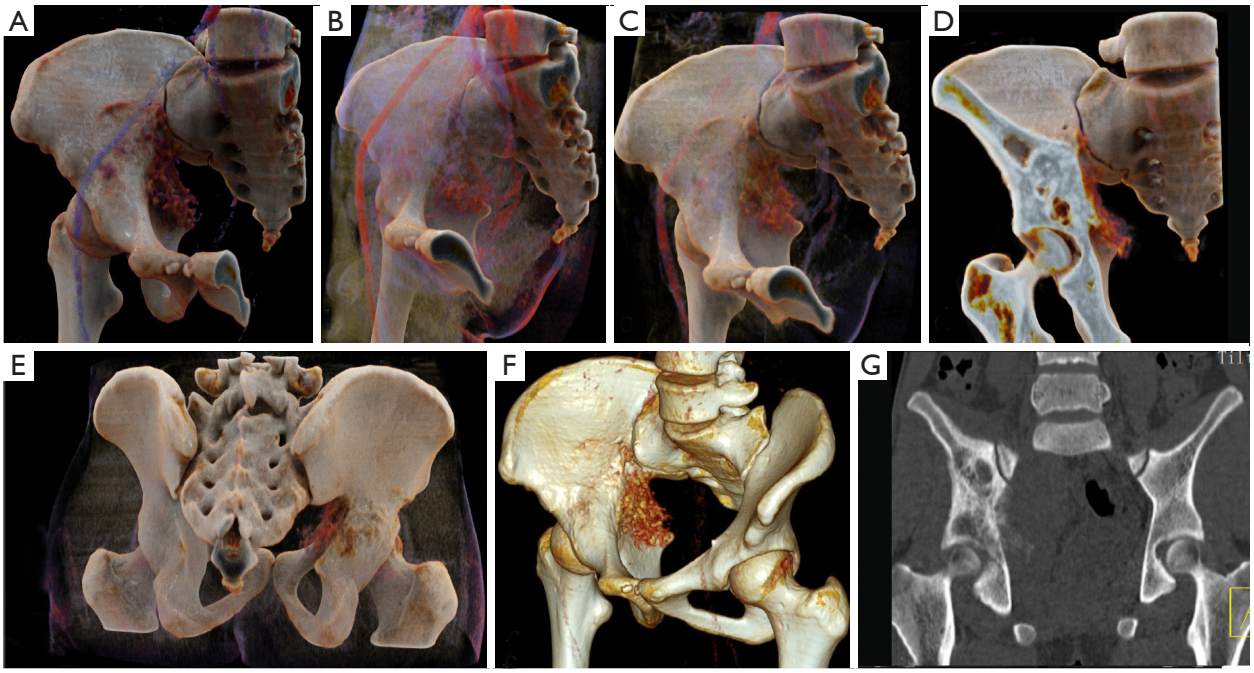

Figure 5 A 17-year-old male presented with a right hip mass that had gradually increased for 1 year. CR (A-E), VR (F) and 2D CT image (G) show the right iliac bone destruction. The tumor had an abundant blood supply, and the sacroiliac joint was not involved. CT, computed tomography; CR, cinematic rendering; VR, volume rendering.

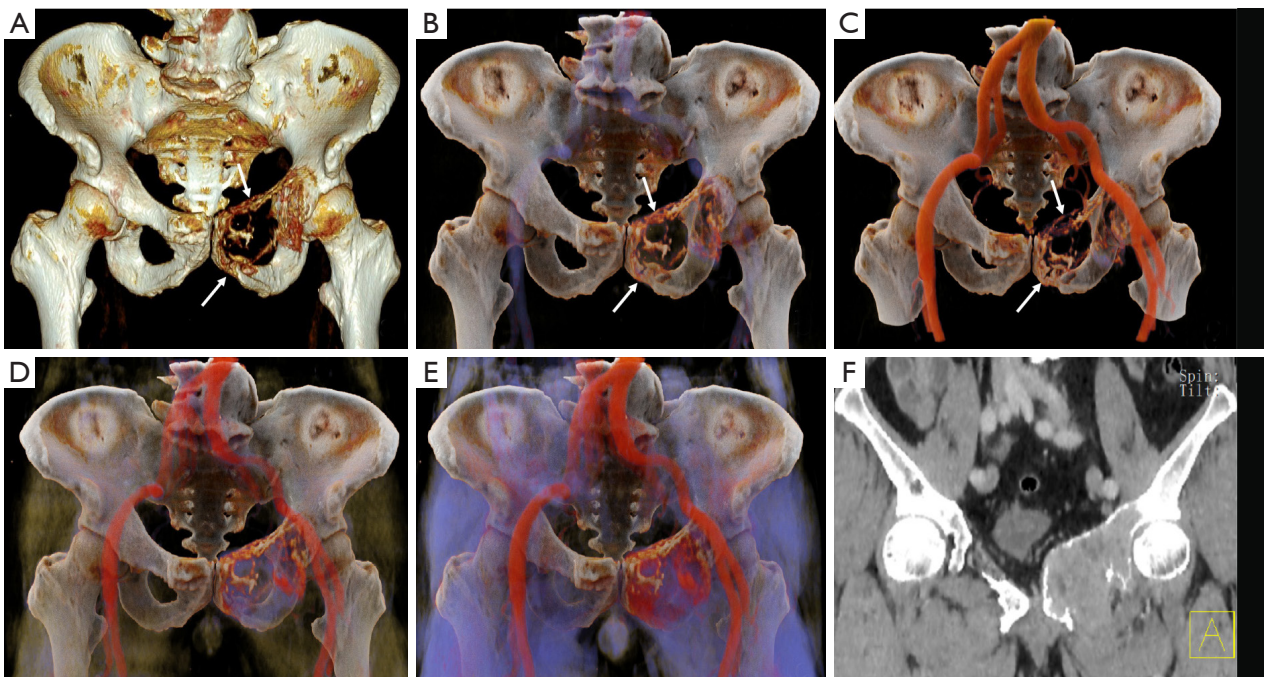

Figure 6 A 61-year-old male with left hip pain for 6 months. VR (A), CR (B-E) and a 2D CT image (F) demonstrate osteolytic destruction of the left acetabulum and pubic bone and the formation of soft tissue masses. CR dynamically shows tumor enhancement of the tumor through different window adjustment techniques. CR shows details of bone destruction more clearly than VR (white arrows). CT, computed tomography; CR, cinematic rendering; VR, volume rendering.

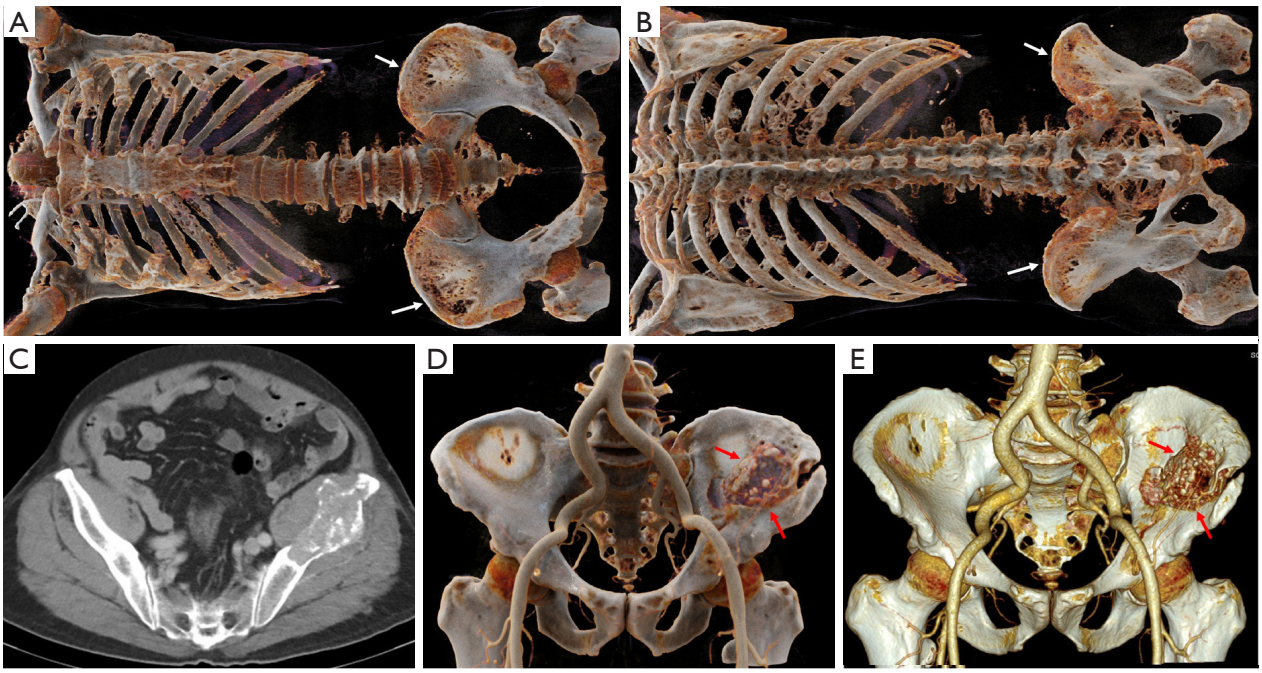

Figure 7 (A,B) CR. A 65-year-old female presented with pain in the back of the waist for 2 months that became gradually aggravated. Diffuse, "punched-out" osteolytic lesions are noted throughout the thoracic and lumbar vertebra, ribs and pelvis (white arrows indicate iliac wing destruction). (C-E) A 67-year-old male presented with left hip pain for more than 4 years that was aggravated for 1 month. The left ilium body and wing exhibit slightly expansive, osteolytic and extensive bone destruction with a large soft-tissue mass (C). Numerous stripe calcifications can be observed in CR (D) and VR (E) (red arrows), and pathological fractures of the ilium are visible around the mass. CR, cinematic rendering; VR, volume rendering.

rim, with tumor calcification observed in 50% to 60% of cases (16). CR and VR can both be used to observe lesions from different angles and remove areas of occlusions, but CR offers more detailed and photorealistic images (*Figure 9*).

Benign pelvic tumors

Osteochondroma

Osteochondroma is a common benign bone tumor that often occurs in long tubular bones, especially in the femur, humerus and tibia. The knee, ilium, hand and foot are also common locations. Osteochondroma is usually asymptomatic, and symptoms appear when the tumor grows and compresses the blood vessels and nervous system. The osteochondromas of the pubic and ischia may compress the urogenital structures. Radiographically, osteochondroma appears as a lesion composed of cortical and medullary bone protruding from, and continuous with, the underlying bone (17). The bony continuous area between the mother bone and osteochondroma can be wide or narrow (*Figures 10,11*). CR can realistically display the relationship between the tumor and the parent bone from different views. Osteochondroma grows slowly, but if it grows too fast or suddenly increases, it may become chondrosarcoma (*Figure 12*).

Giant cell tumor (GCT)

GCTs mainly occur in young patients between 20 and 30 years of age and exhibit a female predominance (16). GCT rarely occurs in the pelvis but when it does it is mainly found in the sacrum. GCT often exhibits osteolytic destruction, cortical expansion with a cortical shell and bony separation. GCTs have a well-defined border, no hardening of the rim, and eccentric growth that can extend to adjacent articular surfaces, often occurring at the end of the bone with closed physes (18). Due to secondary aneurysmal bone cysts (ABCs), GCTs can also contain liquid-liquid levels which typically indicate hemorrhage with sedimentation (15).

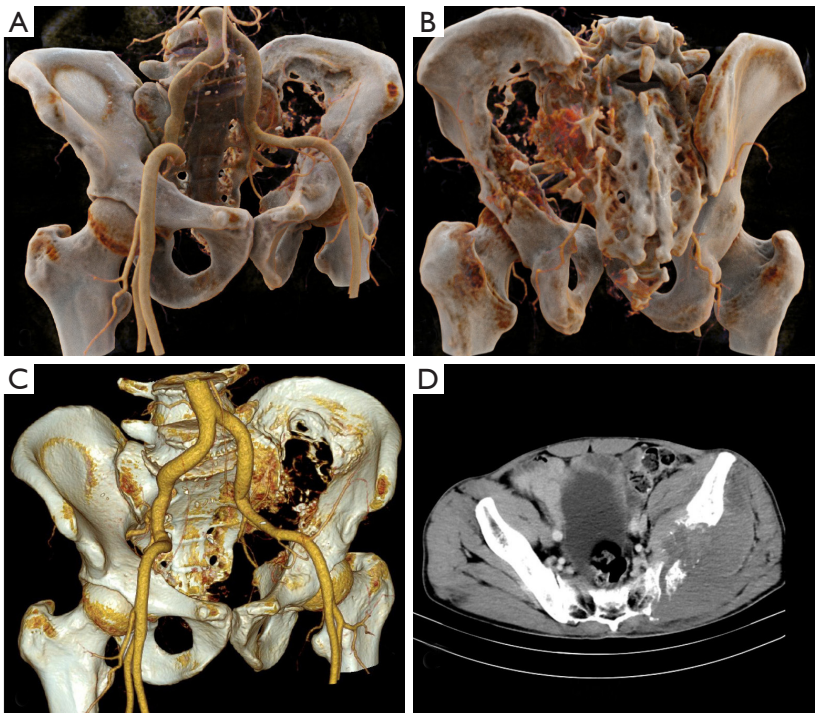

Figure 8 A 48-year-old male presented with left hip and lower limb pain for 8 months that was aggravated with swelling for 6 months. The left iliac bone, acetabulum and sacral bone show extensive moth-eaten osteolysis and no reactive sclerosis, with an irregular soft tissue mass (A-C). CR (A and B) demonstrated more details than VR (C). The lesion was characterized by inhomogeneous enhancement (D). CR, cinematic rendering; VR, volume rendering.

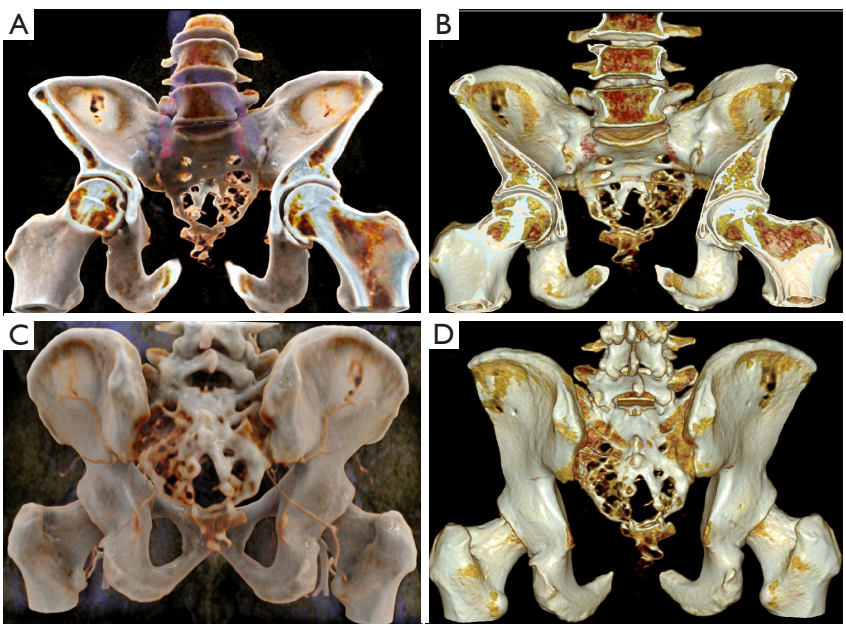

Figure 9 Front view (A and B) and back view (C and D). A 55-year-old male presented with lumbosacral pain for more than 6 months that was aggravated for 1 week. CR (A and C) and VR (B and D) presented 2–4 sacral bony destruction sites with a residual bone crest and calcification inside. CR, cinematic rendering; VR, volume rendering.

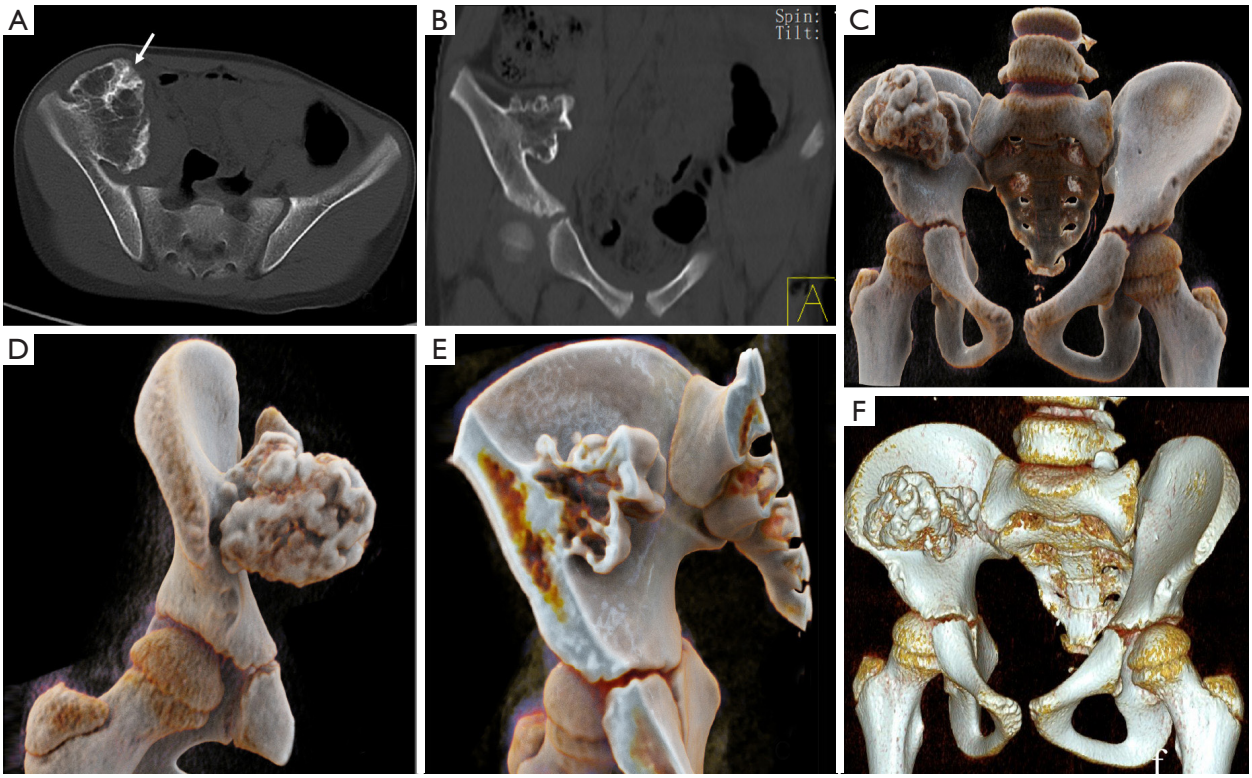

Figure 10 (A-F) Benign solitary osteochondroma of the ilium in an 8-year-old child. Axial CT scan (A) and coronal position reconstruction (B), CR (C-E) and VR (F) images show the marrow and cortical continuity of an osteochondroma and the underlying illium. The lump is cauliflower-like, and the edge is partially hardened (arrow). CT, computed tomography; CR, cinematic rendering; VR, volume rendering.

Imaging findings of GCTs in the pelvis are less likely to demonstrate the classical appearance of those in the long bones. CR can adjust the display parameters to provide information on different tissue types and better visualize soft tissue and bone. CR reconstruction can be performed using different transparencies of the soft tissue and can display tumor detail and enhancement (*Figure 13*). As with MPR and VRT, CR can tailor the lesion using the clip plane in any direction to better display the internal structure and overall panorama of the lesion.

Chondroblastoma (CB)

CB is a rare benign tumor that accounts for less than 1% of all primary bone tumors (19). CB typically occurs in the proximal humeral epiphysis or femoral and tibial condyles, and is rarely located in the pelvis. CB often occurs in young people, generally in adolescents, with a male to female ratio of 2:1 (20,21). *Figure 14* provides two rare cases of pelvic CB. Imaging findings demonstrate a well-defined eccentric oval or round lytic lesion with some expansion and a thin sclerotic rim. Punctate and flocculent calcification is often noted in the center of mass, and the mass occasionally contains fluid levels. Imaging features may be similar with chondrosarcoma, but the age of onset is younger.

Fibrous dysplasia (FD)

FD is a tumor-like lesion that occurs in the bone. It refers to normal marrow and cancellous bone in any part of the body, replaced by abnormal fibrous tissue and immature trabecular bone, leading to osteolytic lesion, fracture, and deformity. The disease manifests as monostotic bone or polyostotic bones. Pelvic bones are frequently involved in the polyostotic form (22). Radiologically, FD presents as a mild to moderate expansion of marrow with a ground glass appearance, mild sclerotic rim, no periosteal reaction and a soft mass (*Figure 15A,B,C*). Utilizing varying window widths

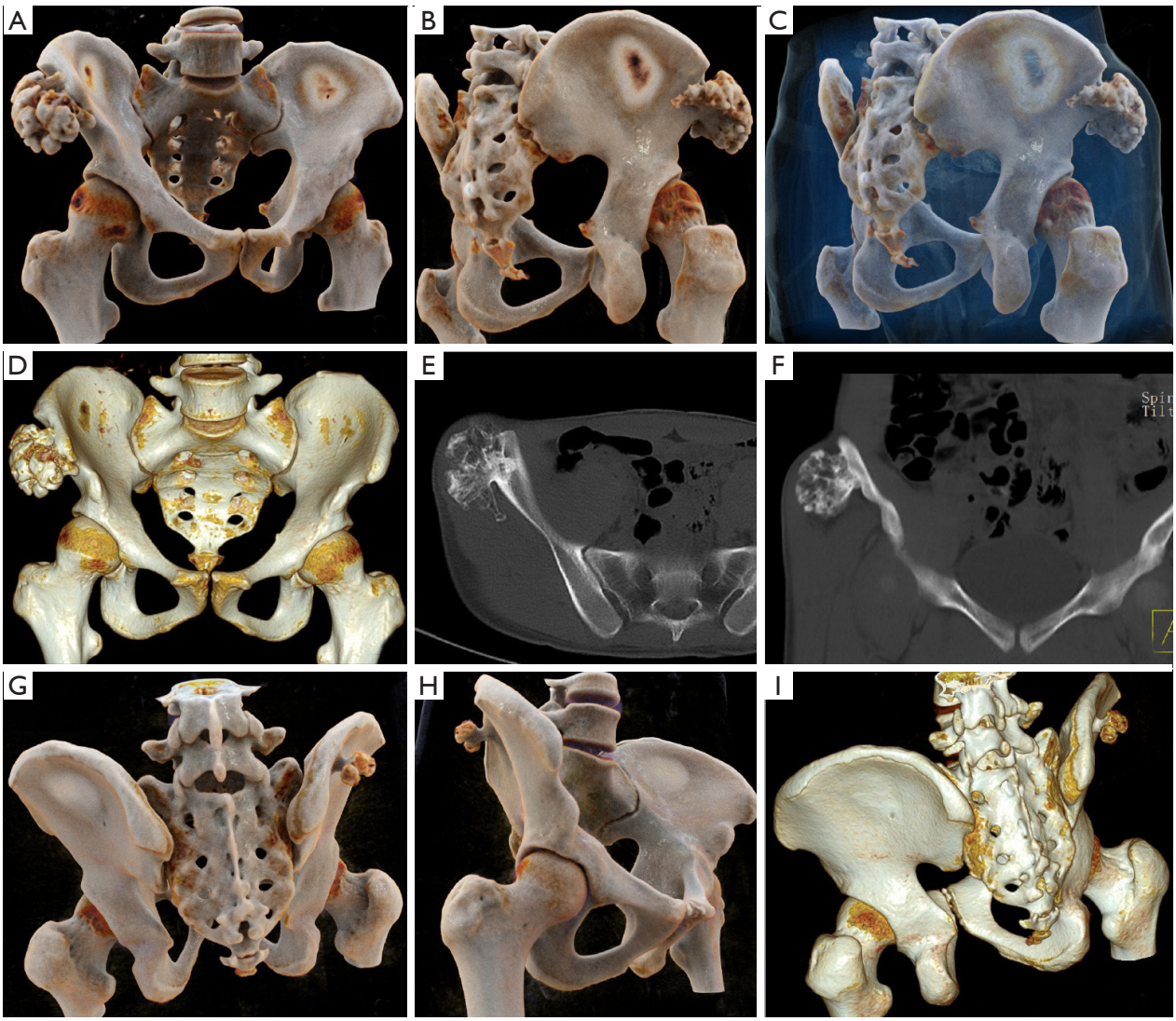

Figure 11 (A-F) A 21-year-old man with osteochondroma of the right ilium for 3 years. CR (A-C), VR (D), axial CT scan (E) and coronal position reconstruction (F) images demonstrate a pedunculated osteochondroma with wide and cortical continuity to the underlying ilium. (G-I) A 15-year-old man with osteochondroma in the posterior of the ilium. CR (G and H) and VR (I) reveal a pedunculated osteochondroma with marrow and cortical continuity to the underlying mother bone. CR, cinematic rendering; VR, volume rendering.

and cut planes of CR, it is possible to display the internal structure of the bone destruction zone (*Figure 15D,E,F,G*). CR provides a better overall appreciation of the degree of lesion and joint deformity.

ABC

ABC is a benign tumor-like lesion that most often occurs in long bones, followed by the pelvis and the spine (23). Primary ABC often occurs under the age of 20, with patients usually presenting with localized pain and swelling. The radiologic features of the lesions show well-defined osteolytic areas with fluid-fluid levels inside the tumor. Bone destruction is marked by expansion with a thinned cortex, and without calcified matrix. At the later stage of development, the outline of the cortex is clear, forming the appearance of the soap bubbles (*Figure 16*).

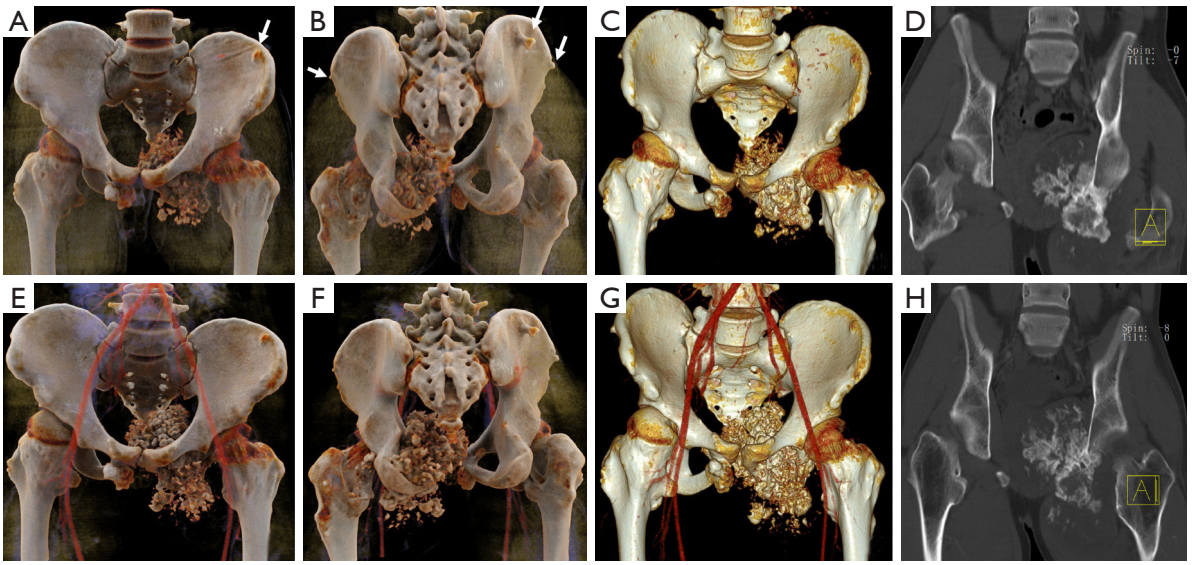

Figure 12 (A-H) A 19-year-old man with multiple osteochondroma for ten years. CR (A and B), VR (C), and CT coronal position reconstruction (D) images demonstrate left sciatic bone destruction and an exogenous lobular mass, with many round and high-density calcifications in the tumor. After 4 months, the tumor was significantly enlarged (E-H), and the pathology confirmed that the tumor became chondrosarcoma. In addition, multiple osteochondromas were observed from different views (arrows). CR (E and F), VR (G), and CT coronal position reconstruction (H). CT, computed tomography; CR, cinematic rendering; VR, volume rendering.

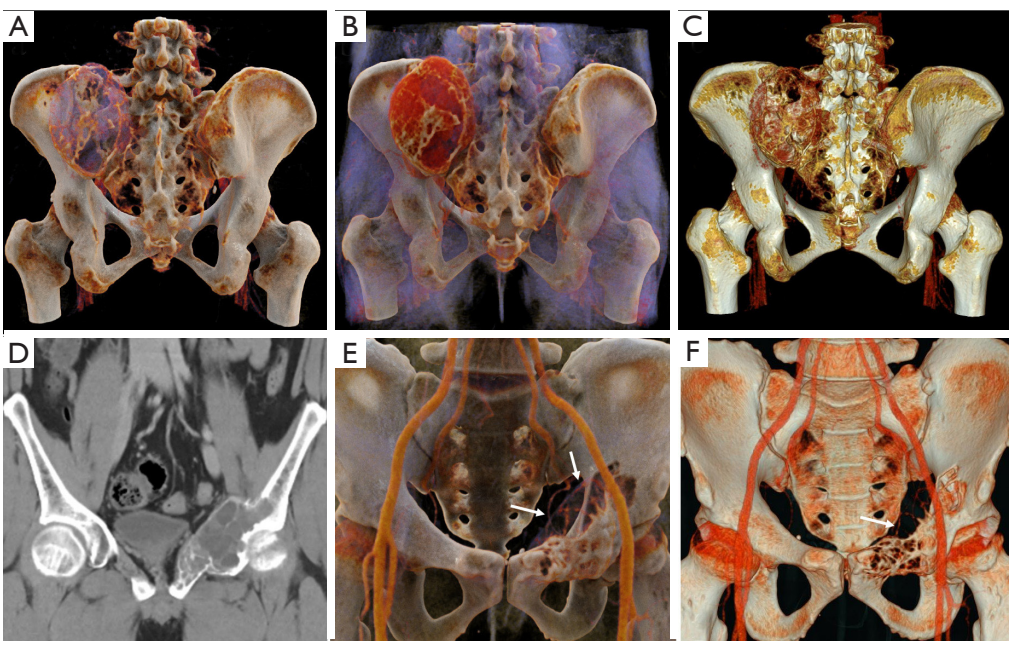

Figure 13 (A-C) A 59-year-old female presented with pain in the left lump and sacrum for one year. CT reveals an expanding destructive lesion in the left iliac and sacrum with a soft tissue mass, and the lesion is located across the sacroiliac joint. CR (A and B) can be performed using different transparencies of the tumor. Numerous intratumoral bony separations are noted in CR and VR (C). The density of the lesion is homogeneous, and the lesion exhibits obvious inhomogeneous enhancement. The CT value is approximately 121 HU. (D-F) A 37-year-old male presented with left hip pain for 1 year that was aggregated for 6 months. The left pubic bone exhibits expansive bone destruction, and liquid-liquid levels are present in the tumor (D). CR (E) and VR (F) can clearly demonstrate bone cortex thinning and multiple bony separations (white arrows). CT, computed tomography; CR, cinematic rendering; VR, volume rendering.

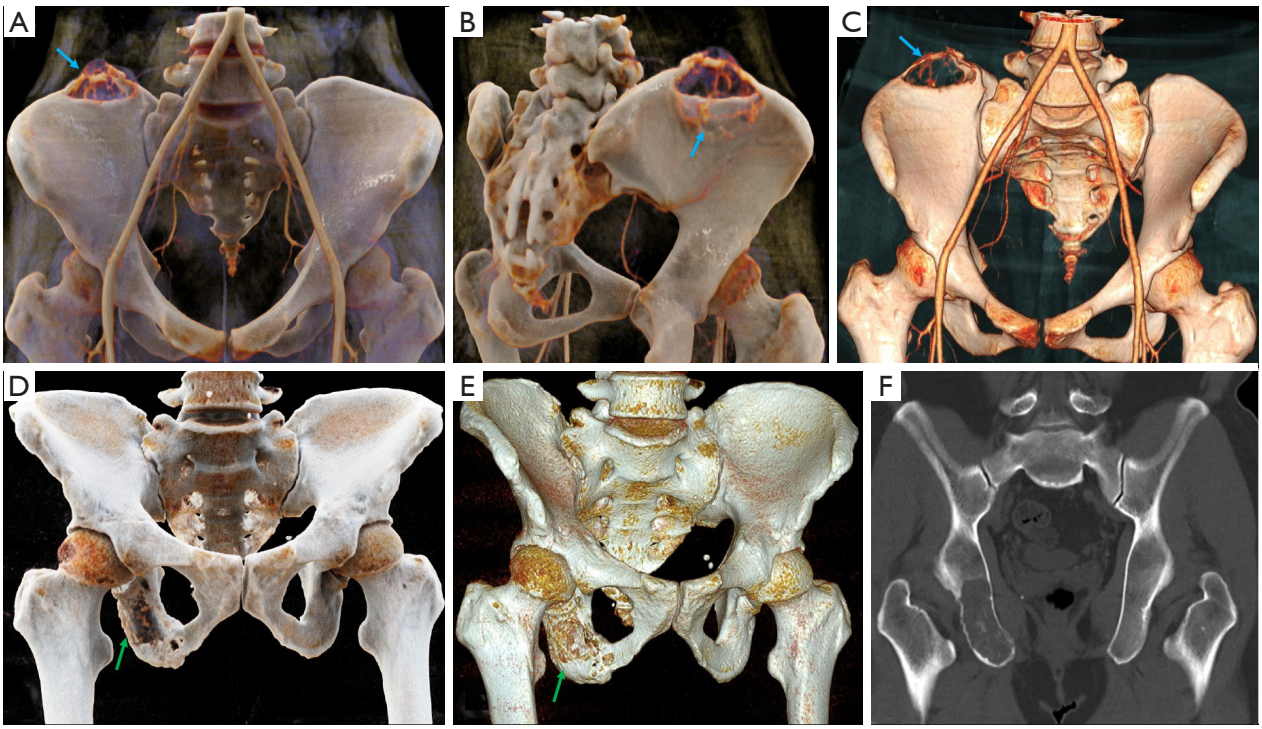

Figure 14 (A-C) A 14-year-old female presented with right iliac pain lasting 5 months. The right iliac wing was moderately expansive, and lytic destruction can be seen in CR (A and B) and VR (C). CR shows that the residual bone crest of bone destruction is superior to that of VR (blue arrows). (D-F) A 46-year-old male presented with right hip and near thigh root pain lasting more than one year. The right ischial bone and acetabulum exhibit moderately expansive destruction in CR (D) and VR (E). The cortex is thinner and discontinuous. The boundary is well defined, and no sclerotic rim is observed (F). CR showed that the internal structure of the bone destruction area was better than that of VR (green arrows). CR, cinematic rendering; VR, volume rendering.

Discussion

In this manuscript, we present a series of primary pelvic tumors highlighting the important differences between potential CR and traditional VR. The most significant difference between CR and VR is that CR uses the global illumination model, which is more complex and can generate more high-quality photorealistic images than the traditional ray-casting model. Although the traditional 2D and 3D play important roles in preoperative plans for pelvic tumors, CR visualization can provide additional value by enhancing the details and photorealism. By adjusting the image window, CR can provide dynamic, continuous observation of the lesion, from its surface to its interior, and photo-realistically and comprehensively display the lesion panorama. Due to the use of complex light-efficient dynamic light patterns (i.e., soft shadows) visual depth perception is improved; in other words, this technique can generate an approximate realistic reconstruction of adjacent and distant spatial structures in different depth planes of an image (3). This unique technological feat cannot be achieved by other traditional radiological methods. By providing high-quality realistic images, CR has helped orthopaedic multidisciplinary teams (MDTs) to develop treatment protocols, thus facilitating patient communication. Indeed, Berger *et al.* (24) found that most radiologists and orthopedic surgeons thought CR images give a more natural and clearer depiction of anatomic structures. Using this technique can improve the exchange of information between clinicians and radiologists. In addition, it is helpful for clinicians to understand the signs of radiology, such as intratumoral bony separations of FD (*Figure 15*) and the soapy-like appearance of ABCs (*Figure 16*).

CR is also helpful for determining the regional location of pelvic tumors, aiding in patient comprehension, facilitating clinical decision making, and promoting the accuracy of 3D-printed models. Three-dimensional high-definition vascular maps of CR can reveal the degree of tumor

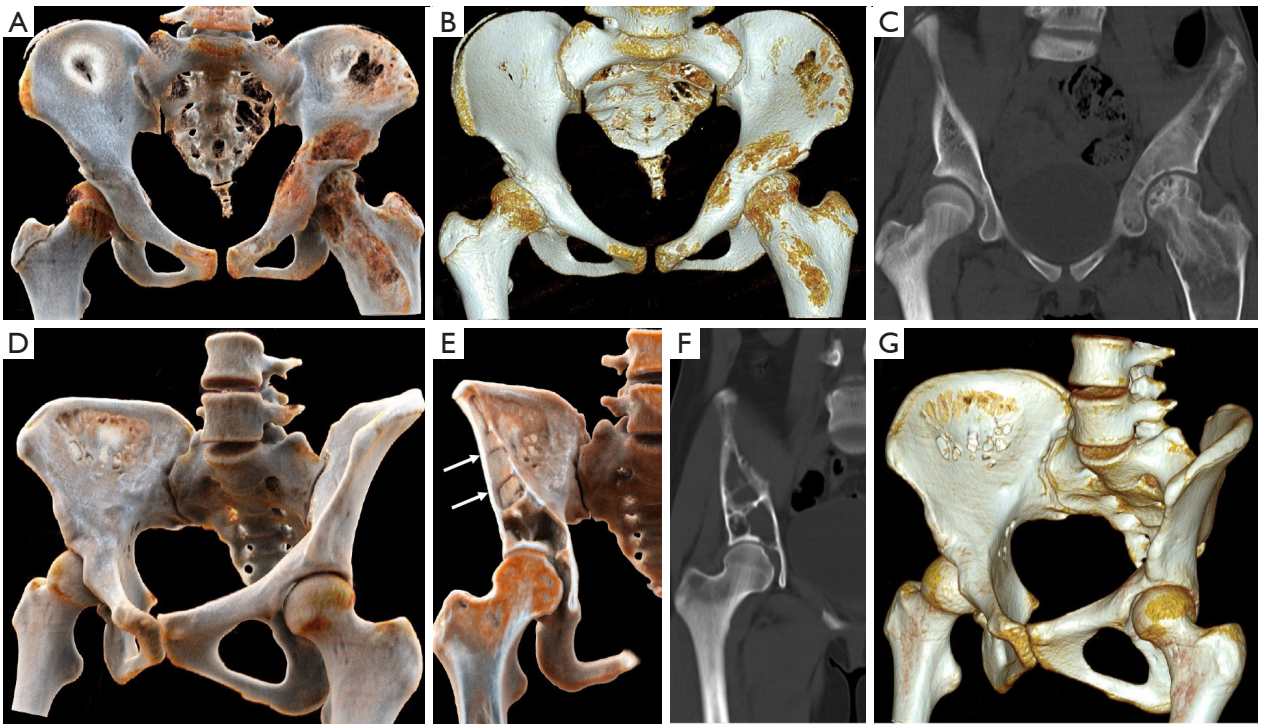

Figure 15 (A-C) Multiple bone fibrous dysplasia (polyostotic). An 11-year-old female presented with lame left lower extremities lasting for 1 year. The left iliac, acetabulum and femur exhibit mixed bone destruction. The lesion is moderately expanded with a mixture of sclerosis, ground-glass, and lytic regions and lacks a sclerotic rim. Deformity of the femoral valgus is clearly visible in CR. (D-G) A 17-year-old female presented with right pelvis fibrous dysplasia (monostotic). The right iliac and acetabulum exhibit well-defined lytic destruction with bony expansion and many bony separations inside. The CR displays the intratumoral bony separations as well (white arrows). A, D, and E are CR images; B and G are VR images; C and F are coronal 2D CT images. CR, cinematic rendering; VR, volume rendering.

invasion, aid in the determination of tumor resectability and determine the revascularization scheme (*Figures 3*,*6*,*8*) (25). Furthermore, the globalized presentation of CR helps surgeons develop personalized preoperative pelvic protocols and pelvic reconstruction protocols. In the process of CR imaging, the radiologist or surgeon needs to interact with the workstation in real time and optimize the appropriate template and window setting, so the pathological features and anatomy can be better displayed according to the situation. In the process of imaging using CR, radiologists and surgeons, by using multi-angle and multi-level observation, can better understand the pathology of the lesions and the spatial relationship with the surrounding tissues, simulating the findings in the surgery and boosting the surgeons' confidence. It may even save time during surgery. In addition, because CR shows details better than traditional 3D imaging, it can accurately display pelvic tumor invasion of blood vessels or joints, which can improve limb salvage rate and prevent excessive damage. At present, diagnosis relies mainly on the traditional method based on plane reconstruction, but the diagnosis of complex diseases may benefit from the flexibility and expressiveness of this new CR technology (26). The textural features of internal heterogeneity and necrosis in large tumors can be optimally displayed through CR (6). Understanding these textural features can aid in disease diagnosis. The various internal morphologies of the tumor bone and calcification noted in the cases in this study were displayed extremely realistically through CR. High-density objects, such as bone, or contrast-enhanced structures, such as blood vessels and hyper-enhanced tumors, e.g., GCT, are ideal for reconstruction through CR and can be represented with high quality in CR. However, in some deep areas where light is easily blocked and in hypo-enhanced lesions, the performance of CR is not outstanding.

In addition to clinical applications, CR can also be used

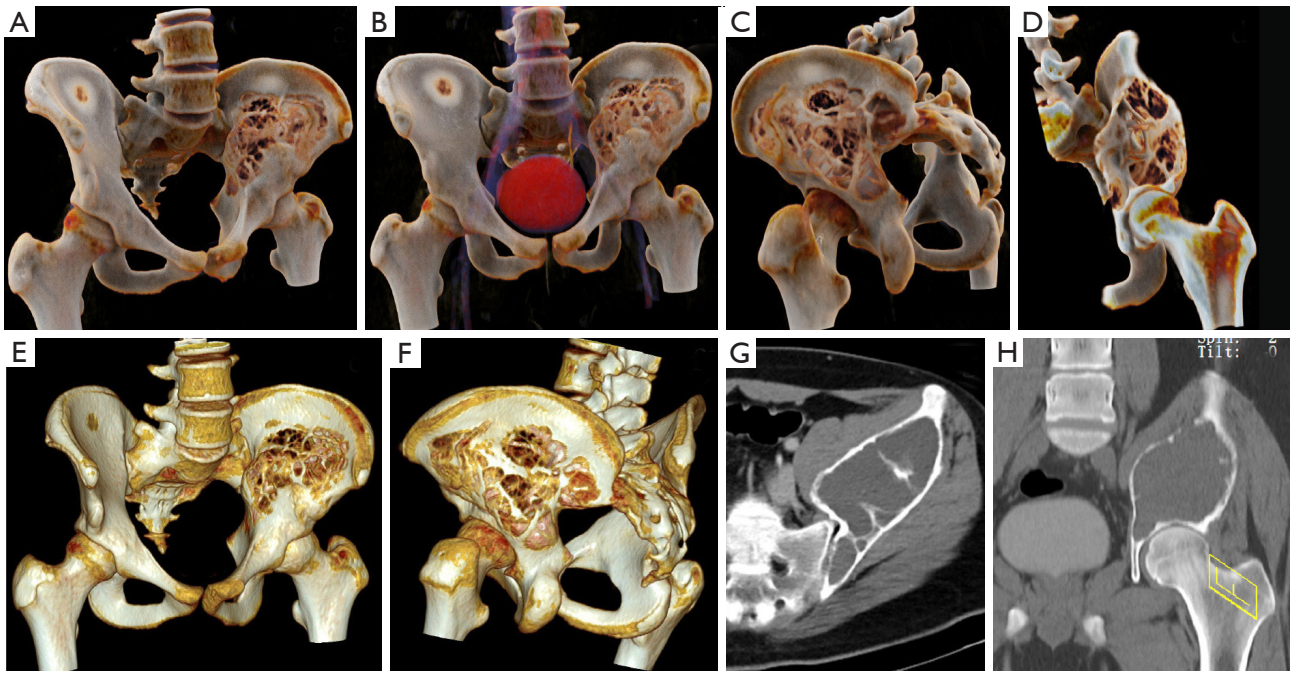

Figure 16 A 14-year-old male with ABC in the ilium. CR (A-D), VR (E and F), and 2D CT (G and H) images demonstrate expanded left iliac bone destruction and a soap bubble-like appearance. The cortex is thin and discontinuous. aneurysmal bone cyst; CT, computed tomography; CR, cinematic rendering; VR, volume rendering.

in medical education. For instance, CR can be applied as a new technique for teaching anatomy. This new teaching method makes it easier for beginners to understand complex anatomical structures while saving cadavers and accelerating the journey from the bench to the bedside. The anatomy of the pelvis revealed by CR in *Figure 1* is a good example of this imaging as an educational aid. In addition, CR has the potential to achieve virtual simulation of layer-by-layer dissection of the anatomy of a human corpse, and the integration of CR into navigation tools and 3D vision labs may partially replace the anatomy curriculum using corpses (3).

Although CR is a new technology, several limitations should be noted. Compared with VR, CR uses more complex algorithms and requires more powerful processors and longer processing times. Second, the shadow effect produced by the global illumination model does make the image photorealistic, but this shadow effect may obscure small lesions and even important pathology. Finally, compared with VRT, CR exhibits no obvious advantage in hypo-enhanced soft tissue tumors and requires further improvements. If CR can integrate the region-growth method, it may achieve better results.

In conclusion, CR is a new and promising imaging technique that exhibits a wide range of uses in the diagnosis of pelvic tumors, tumor division, preoperative planning, and communication with patients. Compared with traditional VR, the main innovation of CR is the ability to present CT volume data more naturally and photo-realistically with a rich and colorful template. When you view these images, you are not only diagnosing a condition but also observing important details.

Acknowledgements

Funding: This study was supported by the National Natural Science Foundation of China (Grant No. 81703155), the Yunnan Applied Basic Research Projects-KMU Joint Special Project [Grant no. 2017FE468(-071)] and the Yunnan Health Training Project of High Level Talents (H-2017005) and the Yunnan Doctoral Student New Scholar Award (2017).

Footnote

Conflicts of Interest: The authors have no conflicts of interest to declare.

References

1. Rowe SP, Johnson PT, Fishman EK. Cinematic rendering of cardiac CT volumetric data: Principles and initial observations. J Cardiovasc Comput Tomogr 2018;12:56-9.
2. Ebert LC, Schweitzer W, Gascho D, Ruder TD, Flach PM, Thali MJ, Ampanozi G. Forensic 3D Visualization of CT Data Using Cinematic Volume Rendering: A Preliminary Study. AJR Am J Roentgenol 2017;208:233-40.
3. Glemser PA, Engel K, Simons D, Steffens J, Schlemmer HP, Orakcioglu B. A New Approach for Photorealistic Visualization of Rendered Computed Tomography Images. World Neurosurg 2018;114:e283-92.
4. Johnson PT, Schneider R, Lugo-Fagundo C, Johnson MB, Fishman EK. MDCT Angiography With 3D Rendering: A Novel Cinematic Rendering Algorithm for Enhanced Anatomic Detail. AJR Am J Roentgenol 2017;209:309-12.
5. Rowe SP, Meyer AR, Gorin MA, Johnson PT, Fishman EK. 3D CT of renal pathology: initial experience with cinematic rendering. Abdom Radiol (NY) 2018. [Epub ahead of print]. doi: 10.1007/s00261-018-1644-7.
6. Rowe SP, Chu LC, Fishman EK. Evaluation of Stomach Neoplasms With 3-Dimensional Computed Tomography: Focus on the Potential Role of Cinematic Rendering. J Comput Assist Tomogr 2018;42:661-6.
7. Rowe SP, Fritz J, Fishman EK. CT evaluation of musculoskeletal trauma: initial experience with cinematic rendering. Emerg Radiol 2018;25:93-101.
8. Rajiah P, Ilaslan H, Sundaram M. Imaging of sarcomas of pelvic bones. Semin Ultrasound CT MR 2011;32:433-41.
9. Ottaviani G, Jaffe N. The epidemiology of osteosarcoma. Cancer Treat Res 2009;152:3-13.
10. Parry MC, Laitinen M, Albergo J, Jeys L, Carter S, Gaston C, Sumathi V, Grimer R. Osteosarcoma of the pelvis. Bone Joint J 2016;98-B:555-63.
11. Donati D, Giacomini S, Gozzi E, Ferrari S, Sangiorgi L, Tienghi A, DeGroot H, Bertoni F, Bacchini P, Bacci G, Mercuri M. Osteosarcoma of the pelvis. Eur J Surg Oncol 2004;30:332-40.
12. Park SK, Lee IS, Cho KH, Lee YH, Yi JH, Choi KU. Osteosarcoma of pelvic bones: imaging features. Clin Imaging 2017;41:59-64.
13. Sun Y, Liu X, Pan S, Deng C, Li X, Guo Q. Analysis of imaging characteristics of primary malignant bone tumors in children. Oncol Lett 2017;14:5801-10.
14. Bloem JL, Reidsma, II. Bone and soft tissue tumors of hip and pelvis. Eur J Radiol 2012;81:3793-801.
15. Ong KO, Ritchie DA. Pictorial essay: tumours and pseudotumours of sacrum. Can Assoc Radiol J 2014;65:113-20.
16. Gerber S, Ollivier L, Leclere J, Vanel D, Missenard G, Brisse H, de Pinieux G, Neuenschwander S. Imaging of sacral tumours. Skeletal Radiol 2008;37:277-89.
17. Murphey MD, Choi JJ, Kransdorf MJ, Flemming DJ, Gannon FH. Imaging of osteochondroma: variants and complications with radiologic-pathologic correlation. Radiographics 2000;20:1407-34.
18. Chakarun CJ, Forrester DM, Gottsegen CJ, Patel DB, White EA, Matcuk GR, Jr. Giant cell tumor of bone: review, mimics, and new developments in treatment. Radiographics 2013;33:197-211.
19. Suneja R, Grimer RJ, Belthur M, Jeys L, Carter SR, Tillman RM, Davies AM. Chondroblastoma of bone: long-term results and functional outcome after intralesional curettage. J Bone Joint Surg Br 2005;87:974-8.
20. Lin PP, Thenappan A, Deavers MT, Lewis VO, Yasko AW. Treatment and prognosis of chondroblastoma. Clin Orthop Relat Res 2005;438:103-9.
21. De Mattos CB, Angsanuntsukh C, Arkader A, Dormans JP. Chondroblastoma and chondromyxoid fibroma. J Am Acad Orthop Surg 2013;21:225-33.
22. Ozsen M, Yalcinkaya U, Bilgen MS, Yazici Z. Fibrous Dysplasia: Clinicopathologic Presentation of 36 Cases. Turk Patoloji Derg 2018;34:234-41.
23. Motamedi K, Seeger LL. Benign bone tumors. Radiol Clin North Am 2011;49:1115-34, v.
24. Berger F, Ebert L, Kubik-Huch R, Eid K, Thali M, Niemann T. Application of Cinematic Rendering in Clinical Routine CT Examination of Ankle Sprains. AJR Am J Roentgenol 2018;211:887-90.
25. Chu LC, Johnson PT, Fishman EK. Cinematic rendering of pancreatic neoplasms: preliminary observations and opportunities. Abdom Radiol (NY) 2018. [Epub ahead of print]. doi: 10.1007/s00261-018-1559-3.
26. Comaniciu D, Engel K, Georgescu B, Mansi T. Shaping the future through innovations: From medical imaging to precision medicine. Med Image Anal 2016;33:19-26.

Cite this article as: Yang J, Li K, Deng H, Feng J, Fei Y, Jin Y, Liao C, Li Q. CT cinematic rendering for pelvic primary tumor photorealistic visualization. Quant Imaging Med Surg 2018;8(8):804-818. doi: 10.21037/qims.2018.09.21